Quantification and Reduction of Uncertainties Associated with Biogeochemistry–Earth System Feedbacks

Forrest M. Hoffman[1], James T. Randerson[2], William J. Riley[3], J. Keith Moore[2], Michael L. Goulden[2], Weiwei Fu[2], Charles D. Koven[3], Abigail L. S. Swann[4], Natalie M. Mahowald[5], Keith Lindsay[6], Ernesto Muñoz[6], and Gordon B. Bonan[6]

[1]Oak Ridge National Laboratory, [2]University of California Irvine, [3]Lawrence Berkeley National Laboratory, [4]University of Washington Seattle, [5]Cornell University, and [6]National Center for Atmospheric Research

ACME Coupled Biogeochemistry (CBGC) Science Presentation

June 27, 2017

Research Questions

Question 1

How well do Earth System Models (ESMs) simulate the observed distribution of anthropogenic carbon in atmosphere, ocean, and land reservoirs?

Research Questions

Question 1

How well do Earth System Models (ESMs) simulate the observed distribution of anthropogenic carbon in atmosphere, ocean, and land reservoirs?

Question 2

Can contemporary atmospheric CO_2 observations be used to constrain future CO_2 projections?

Research Questions

Question 1

How well do Earth System Models (ESMs) simulate the observed distribution of anthropogenic carbon in atmosphere, ocean, and land reservoirs?

Question 2

Can contemporary atmospheric CO_2 observations be used to constrain future CO_2 projections?

Question 3

To what degree do the effects of climate change due to warming and CO_2 fertilization in isolation combine linearly?

Observed Carbon Accumulation Since 1850

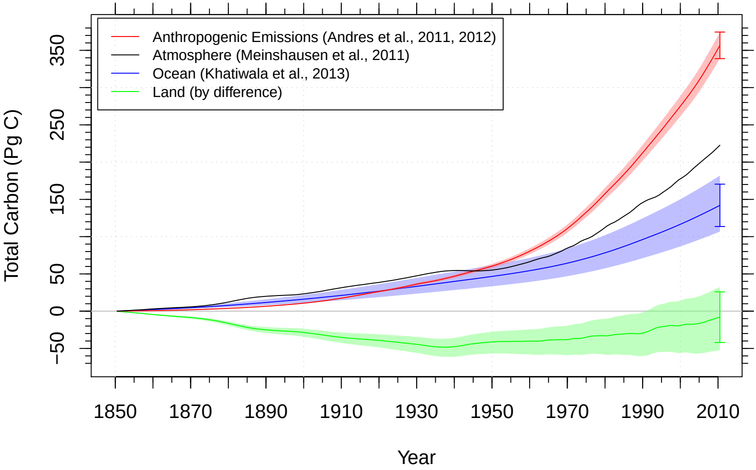

Observational estimates of anthropogenic carbon emissions (excluding land use change) and accumulation in atmosphere, ocean, and land reservoirs for 1850–2010. Atmosphere carbon is a fusion of Law Dome ice core CO_2 observations, the Keeling Mauna Loa record, and more recently the NOAA GMD global surface average, integrated for the purpose of forcing IPCC models. Total land flux is computed by mass balance as follows:

$$\Delta C_L = \sum_i F_i - \Delta C_A - \Delta C_O.$$

15 fully-prognostic ESMs that performed CMIP5 emissions-forced simulations

Model	Modeling Center
BCC-CSM1.1	Beijing Climate Center, China Meteorological Administration, CHINA
BCC-CSM1.1(m)	Beijing Climate Center, China Meteorological Administration, CHINA
BNU-ESM	Beijing Normal University, CHINA
CanESM2	Canadian Centre for Climate Modelling and Analysis, CANADA
CESM1-BGC	Community Earth System Model Contributors, NSF-DOE-NCAR, USA
FGOALS-s2.0	LASG, Institute of Atmospheric Physics, CAS, CHINA
GFDL-ESM2g	NOAA Geophysical Fluid Dynamics Laboratory, USA
GFDL-ESM2m	NOAA Geophysical Fluid Dynamics Laboratory, USA
HadGEM2-ES	Met Office Hadley Centre, UNITED KINGDOM
INM-CM4	Institute for Numerical Mathematics, RUSSIA
IPSL-CM5A-LR	Institut Pierre-Simon Laplace, FRANCE
MIROC-ESM	Japan Agency for Marine-Earth Science and Technology, Atmosphere and Ocean Research Institute (University of Tokyo), and National Institute for Environmental Studies, JAPAN
MPI-ESM-LR	Max Planck Institute for Meteorology, GERMANY
MRI-ESM1	Meteorological Research Institute, JAPAN
NorESM1-ME	Norwegian Climate Centre, NORWAY

CMIP5 Long-Term Experiments

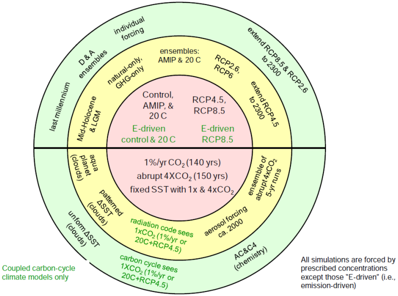

Emissions for Historical + RCP 8.5 Simulations

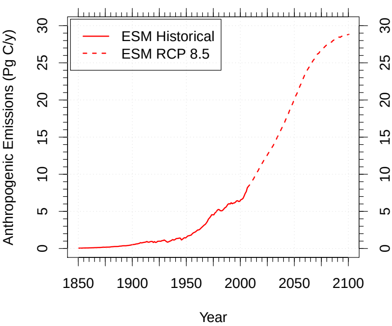

(a) Most ESMs exhibited a high bias in predicted atmospheric CO_2 mole fraction, which ranged from 357–405 ppm at the end of the historical period (1850–2005).

(b) The multi-model mean was biased high from 1946 throughout the 20th century, ending 5.6 ppm above the observed value of 378.8 ppm in 2005.

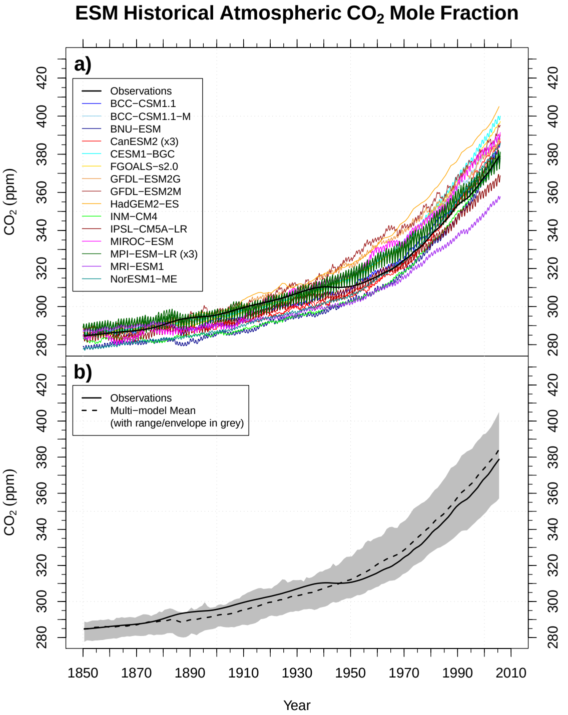

Model inventory comparison with Khatiwala et al. (2013)

Once normalized by their atmospheric carbon inventories, most ESMs exhibited a low bias in anthropogenic ocean carbon accumulation through 2010.

The same pattern holds for the Sabine et al. (2004) inventory derived using the ΔC* separation technique.

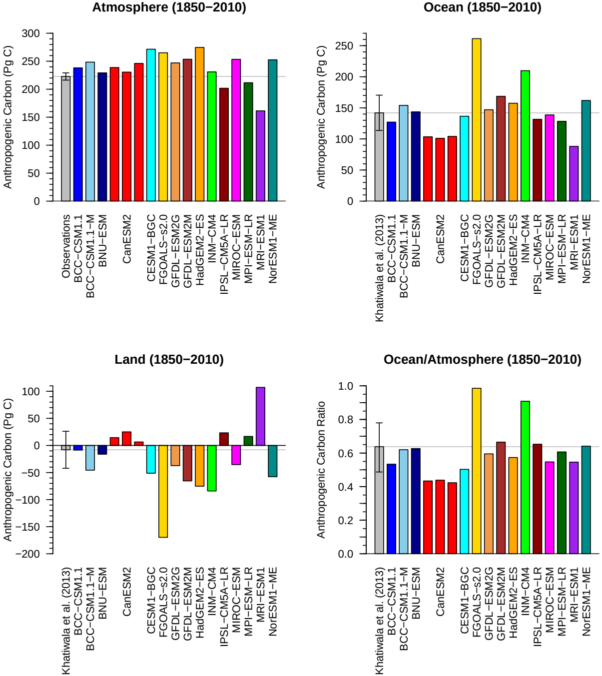

(a) Ocean inventory estimates had a fairly persistent ordering during the second half of the 20th century.

(b) ESMs exhibited a wide range of land carbon accumulation responses to increasing CO_2 and land use change, ranging from a net source of 170 Pg C to a sink of 107 Pg C in 2010.

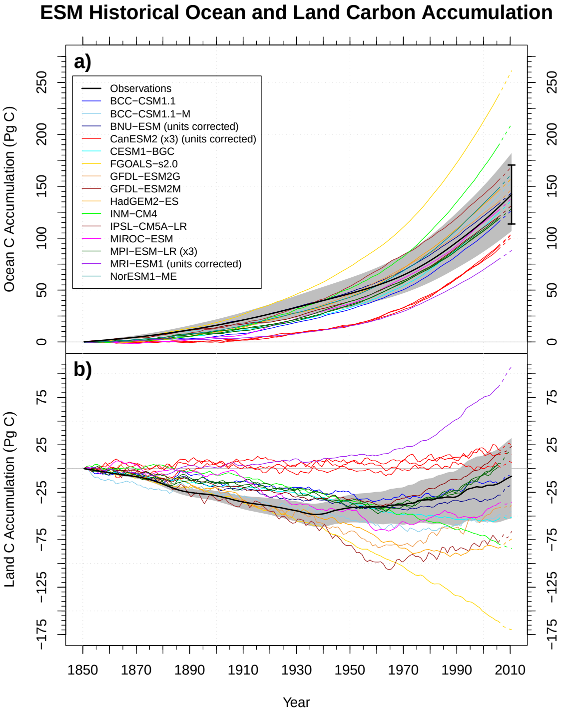

Question 1

How well do Earth System Models (ESMs) simulate the observed distribution of anthropogenic carbon in atmosphere, ocean, and land reservoirs?

- Most ESMs exhibited a high bias in predicted atmospheric CO_2 mole fraction, ranging from 357–405 ppm in 2005.
- The multi-model mean atmospheric CO_2 mole fraction was biased high from 1946 onward, ending 5.6 ppm above observations in 2005.
- Once normalized by atmospheric carbon accumulation, most ESMs exhibited a low bias in ocean accumulation in 2010.
- ESMs predicted a wide range of land carbon accumulation in response to increasing CO_2 and land use change, ranging from -170–107 Pg C in 2010.

Question 2

Can contemporary atmospheric CO_2 observations be used to constrain future CO_2 projections?

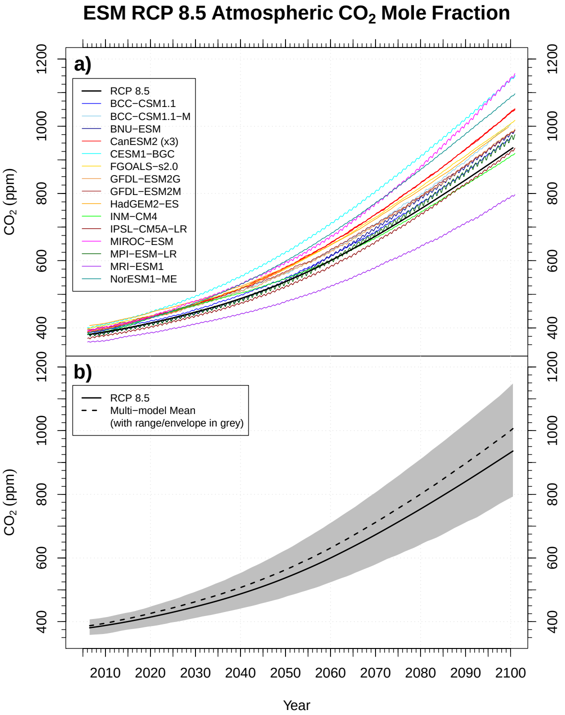

Reducing Uncertainties Using Observations

To reduce feedback uncertainties using contemporary observations,

1. there must be a relationship between contemporary variability and future trends on longer time scales within the model, and

Reducing Uncertainties Using Observations

To reduce feedback uncertainties using contemporary observations,

1. there must be a relationship between contemporary variability and future trends on longer time scales within the model, and
2. it must be possible to constrain contemporary variability in the model using observations.

Reducing Uncertainties Using Observations

To reduce feedback uncertainties using contemporary observations,

1. there must be a relationship between contemporary variability and future trends on longer time scales within the model, and
2. it must be possible to constrain contemporary variability in the model using observations.

Example #1

Hall and Qu (2006) evaluated the strength of the springtime snow albedo feedback (SAF; $\Delta\alpha_s/\Delta T_s$) from 17 models used for the IPCC AR4 and compared them with the observed springtime SAF from ISCCP and ERA-40 reanalysis.

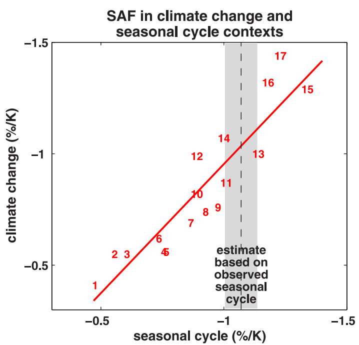

Reducing Uncertainties Using Observations

To reduce feedback uncertainties using contemporary observations,

1. there must be a relationship between contemporary variability and future trends on longer time scales within the model, and
2. it must be possible to constrain contemporary variability in the model using observations.

Example #2

Cox et al. (2013) used the observed relationship between the CO_2 growth rate and tropical temperature as a constraint to reduce uncertainty in the land carbon storage sensitivity to climate change (γ_L) in the tropics using C^4MIP models.

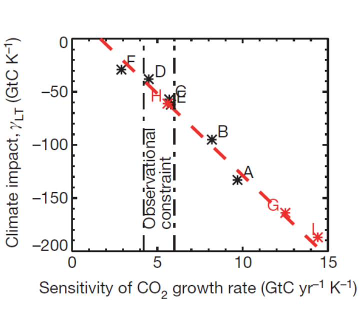

I developed a new emergent constraint from carbon inventories.

A relationship exists between contemporary and future atmospheric CO_2 levels over decadal time scales because carbon model biases persist over decadal time scales.

Observed contemporary atmospheric CO_2 mole fraction is represented by the vertical line at 384.6 ± 0.5 ppm.

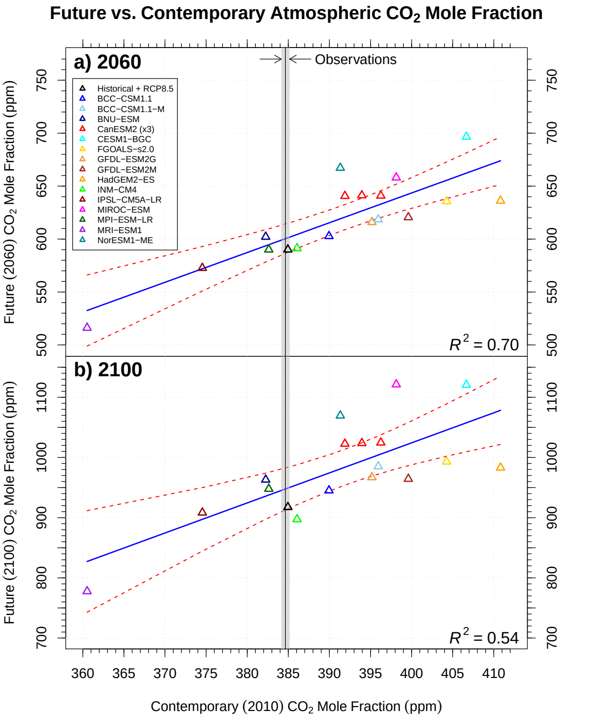

Removing pre-industrial CO_2 mole fraction biases from models, we found the relationship held, confirming the robustness of our result.

Observed contemporary anthropogenic atmospheric carbon inventory is represented by the vertical line at 213.4 ± 6.5 Pg C, which incorporates 1850 CO_2 mole fraction uncertainties.

Adding uncertainties from fossil fuel emissions increased the uncertainty to ± 12.7 Pg C.

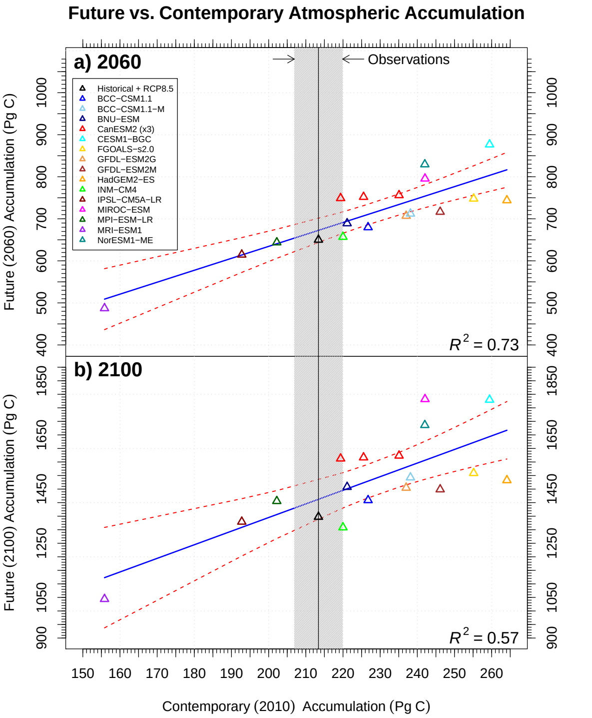

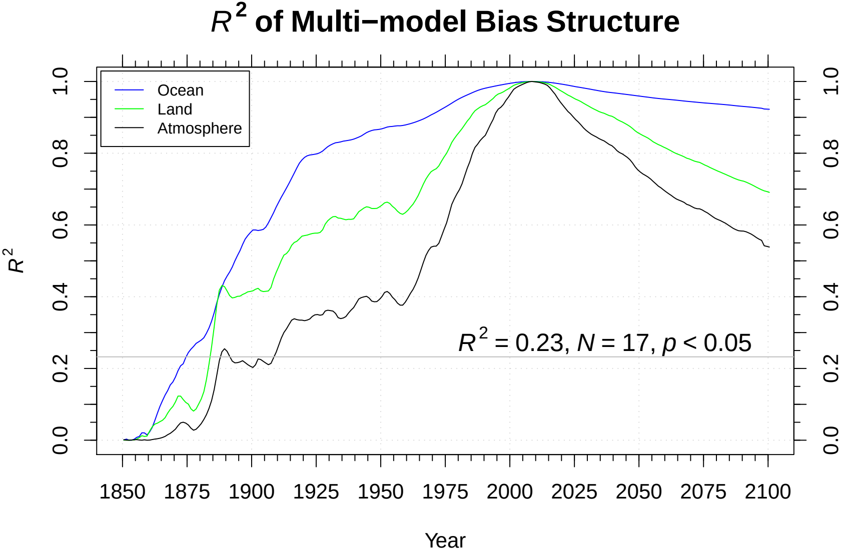

The coefficients of determination (R^2) for the multi-model bias structure relative to the set of CMIP5 model atmospheric CO_2 mole fractions (black), and oceanic (blue) and land (green) anthropogenic carbon inventories in 2010. Atmospheric CO_2 mole fractions are statistically significant for 1910–2100. Bias persistence was highest for the ocean, followed by land, and then by the atmosphere.

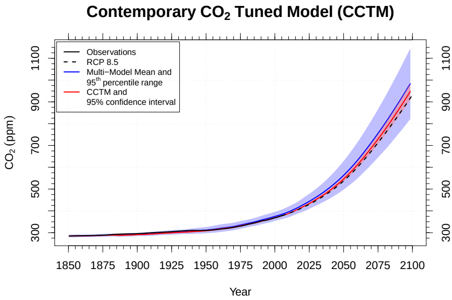

I used this regression to create a contemporary CO_2 tuned model (CCTM) estimate of the atmospheric CO_2 trajectory for the 21st century.

- Peak probability densities of CO_2 mole fraction predictions were lower for the CCTM than the multi-model means.
- The ranges of uncertainty were smaller by almost a factor of 6 at 2060 and almost a factor of 5 at 2100.

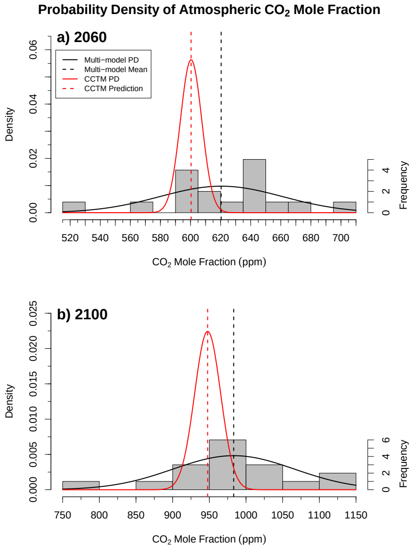

Best estimate using Mauna Loa CO_2

At 2060: 600 ± 14 ppm, 21 ppm below the multi-model mean

At 2100: 947 ± 35 ppm, 32 ppm below the multi-model mean

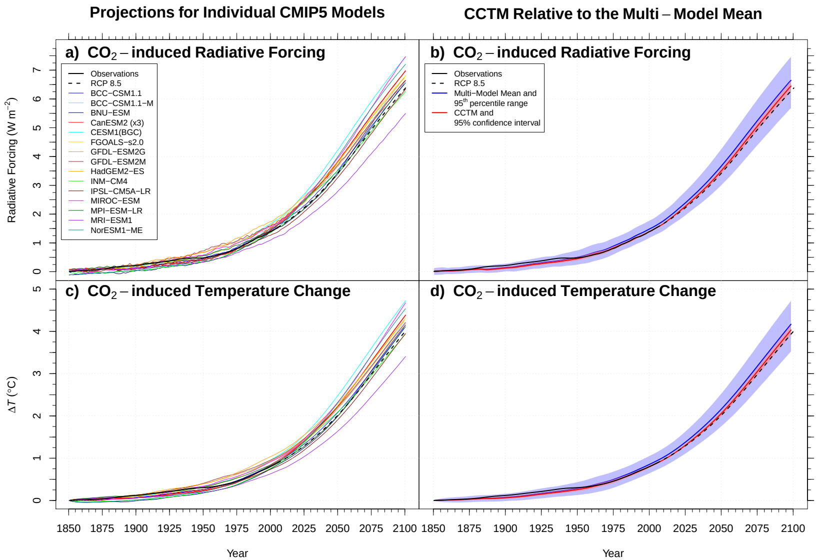

I calculated the CO_2 radiative forcing and used an impulse response function (tuned to the mean transient climate response of CMIP5 models) to equitably compute the resulting CO_2-induced temperature change (ΔT_{CO_2}) for models and the CCTM. The CO_2 biases for individual models contributed to ΔT_{CO_2} biases of -0.7°C to $+0.6^\circ$C by 2100, relative to the CCTM estimate.

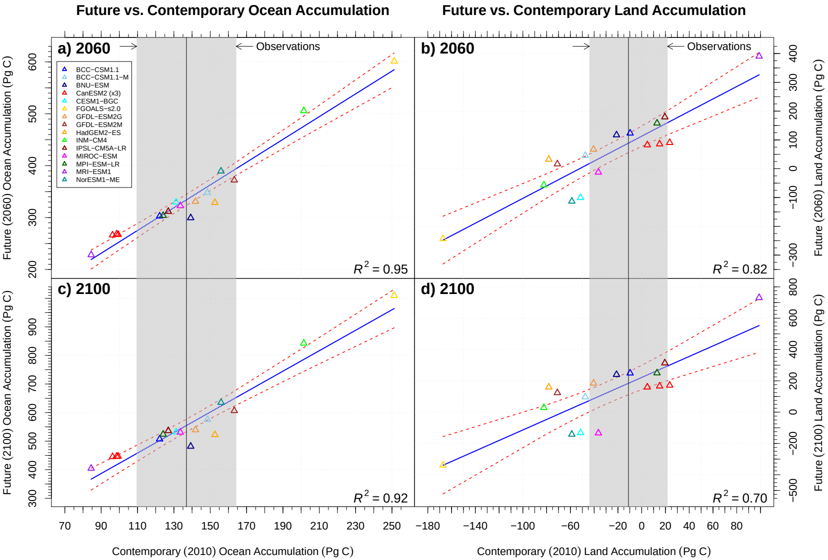

I also developed a multi-model constraint on the evolution of ocean and land anthropogenic inventories. Since observational uncertainties are higher for ocean and land, uncertainties in future estimates cannot be reduced as much as for atmospheric CO_2.

Question 2

Can we use contemporary CO_2 observations to constrain future CO_2 projections?

- Yes.
- I developed a new emergent constraint from anthropogenic carbon inventories in atmosphere, ocean, and land reservoirs.
- Land and ocean processes contributing to contemporary carbon cycle biases persist over decadal timescales.
- I used the relationship between contemporary and future atmospheric CO_2 levels to create a contemporary CO_2 tuned model (CCTM) estimate for the 21st century.
  - At 2060: 600 ± 14 ppm, 21 ppm below the multi-model mean.
  - At 2100: 947 ± 35 ppm, 32 ppm below the multi-model mean.
- Uncertainties in future climate predictions may be reduced by improving models to match the long-term time series of CO_2 from Mauna Loa and other monitoring stations.

Implications of CO_2 Biases in ESMs

- Most of the model-to-model variability of CO_2 in the 21[st] century was traced to biases that existed at the end of the observational record.
- Future fossil fuel emissions targets designed to stabilize CO_2 levels would be too low if estimated from the multi-model mean of ESMs.
- Models could be improved through **extensive comparison with sustained observations** and **community model benchmarking**.


AGU PUBLICATIONS
JGR
Journal of Geophysical Research: Biogeosciences

RESEARCH ARTICLE
10.1002/2013JG002381

Key Points:
- We analyzed emission-driven simulations from 15 Earth System Models (ESMs)
- Most ESMs had a small positive bias in contemporary atmospheric CO_2 predictions
- We used a linear relationship to create a trajectory of future atmospheric CO_2

Supporting Information:
- Readme
- Supplementary Materials

Correspondence to:
F. M. Hoffman,
forrest@climatemodeling.org

Citation:
Hoffman, F. M., J. T. Randerson, V. K. Arora, Q. Bao, P. Cadule, D. Ji, C. D. Jones, M. Kawamiya, S. Khatiwala, K. Lindsay, A. Obata, E. Shevliakova, K. D. Six, J. F. Tjiputra, E. M. Volodin, and T. Wu (2014), Causes and implications of persistent atmospheric carbon dioxide biases in Earth System Models, *J. Geophys. Res. Biogeosci.*, *119*, 141–162, doi:10.1002/2013JG002381.

Received 13 MAY 2013
Accepted 17 DEC 2013
Accepted article online 19 DEC 2013
Published online 15 FEB 2014

Causes and implications of persistent atmospheric carbon dioxide biases in Earth System Models

F. M. Hoffman[1,2], J. T. Randerson[1], V. K. Arora[3], Q. Bao[4], P. Cadule[5], D. Ji[6], C. D. Jones[7], M. Kawamiya[8], S. Khatiwala[9], K. Lindsay[10], A. Obata[11], E. Shevliakova[12], K. D. Six[13], J. F. Tjiputra[14], E. M. Volodin[15], and T. Wu[16]

[1]Department of Earth System Science, University of California, Irvine, California, USA, [2]Climate Change Science Institute and Computational Earth Sciences Group, Oak Ridge National Laboratory, Oak Ridge, Tennessee, USA, [3]Canadian Center for Climate Modeling and Analysis, Meteorological Service of Canada, Victoria, British Columbia, Canada, [4]State Key Laboratory of Numerical Modeling for Atmospheric Sciences and Geophysical Fluid Dynamics, Institute of Atmospheric Physics, Chinese Academy of Sciences, Beijing, China, [5]Institut Pierre Simon Laplace, Laboratoire des Sciences du Climat et de l'Environnement, Gif sur Yvette CEDEX, France, [6]State Key Laboratory of Earth Surface Processes and Resource Ecology, College of Global Change and Earth System Science, Beijing Normal University, Beijing, China, [7]Hadley Center, U.K. Met Office, Exeter, UK, [8]Research Institute for Global Change, Japan Agency for Marine-Earth Science and Technology, Kanagawa, Japan, [9]Lamont Doherty Earth Observatory, Columbia University, Palisades, New York, USA, [10]Climate and Global Dynamics Division, National Center for Atmospheric Research, Boulder, Colorado, USA, [11]Meteorological Research Institute, Japan Meteorological Agency, Ibaraki, Japan, [12]Geophysical Fluid Dynamics Laboratory, Princeton University, Princeton, New Jersey, USA, [13]Max Planck Institute for Meteorology, Hamburg, Germany, [14]Uni Climate, Uni Research, Bergen, Norway, [15]Institute of Numerical Mathematics, Russian Academy of Science, Moscow, Russia, [16]Climate System Modeling Division, Beijing Climate Center, China Meteorological Administration, Beijing, China

Abstract The strength of feedbacks between a changing climate and future CO_2 concentrations is uncertain and difficult to predict using Earth System Models (ESMs). We analyzed emission-driven simulations—in which atmospheric CO_2 levels were computed prognostically—for historical (1850–2005) and future periods (Representative Concentration Pathway (RCP) 8.5 for 2006–2100) produced by 15 ESMs for the Fifth Phase of the Coupled Model Intercomparison Project (CMIP5). Comparison of ESM prognostic atmospheric CO_2 over the historical period with observations indicated that ESMs, on average, had a small positive bias in predictions of contemporary atmospheric CO_2. Weak ocean carbon uptake in many ESMs contributed to this bias, based on comparisons with observations of ocean and atmospheric anthropogenic carbon inventories. We found a significant linear relationship between contemporary atmospheric CO_2 biases and future CO_2 levels for the multimodel ensemble. We used this relationship to create a contemporary CO_2 tuned model (CCTM) estimate of the atmospheric CO_2 trajectory for the 21st century. The CCTM yielded CO_2 estimates of 600 ± 14 ppm at 2060 and 947 ± 35 ppm at 2100, which were 21 ppm and 32 ppm below the multimodel mean during these two time periods. Using this emergent constraint approach, the likely ranges of future atmospheric CO_2, CO_2-induced radiative forcing, and CO_2-induced temperature increases for the RCP 8.5 scenario were considerably narrowed compared to estimates from the full ESM ensemble. Our analysis provided evidence that much of the model-to-model variation in projected CO_2 during the 21st century was tied to biases that existed during the observational era and that model differences in the representation of concentration-carbon feedbacks and other slowly changing carbon cycle processes appear to be the primary driver of this variability. By improving models to more closely match the long-term time series of CO_2 from Mauna Loa, our analysis suggests that uncertainties in future climate projections can be reduced.

1. Introduction

Anthropogenic emissions of radiatively active greenhouse gases into the atmosphere, especially carbon dioxide (CO_2), are rapidly increasing the burden of these gases and altering the Earth's climate [*IPCC*, 2007; *Raupach and J. G. Canadell*, 2010]. This perturbation of the global carbon cycle is expected to induce feedbacks from the terrestrial biosphere and oceans on future CO_2 concentrations and the climate system. These climate–carbon cycle feedbacks are highly uncertain, difficult to predict, and potentially large [*Denman et al.*, 2007]. Understanding and predicting the strength and direction of feedbacks is critically important

Hoffman, Forrest M., James T. Randerson, Vivek K. Arora, Qing Bao, Patricia Cadule, Duoying Ji, Chris D. Jones, Michio Kawamiya, Samar Khatiwala, Keith Lindsay, Atsushi Obata, Elena Shevliakova, Katharina D. Six, Jerry F. Tjiputra, Evgeny M. Volodin, and Tongwen Wu (2014), Causes and Implications of Persistent Atmospheric Carbon Dioxide Biases in Earth System Models, *J. Geophys. Res. Biogeosci.*, 119(2):141162, doi:10.1002/2013JG002381.

Question 3

To what degree do the effects of climate change due to warming and CO_2 fertilization in isolation combine linearly?

Radiative Forcing for RCPs and ECPs

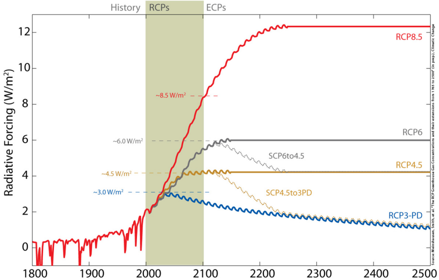

Meinshausen et al. (2011) extended RCP forcings out to 2500.

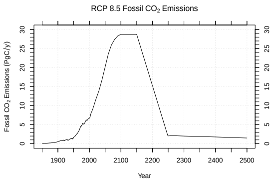

$$\Delta C_O = \beta_O \, \Delta CO_2 + \gamma_O \, \Delta T$$

$$\Delta C_L = \beta_L \, \Delta CO_2 + \gamma_L \, \Delta T$$

$$g = \frac{-\alpha \left(\gamma_O + \gamma_L\right)}{\left(m + \beta_O + \beta_L\right)}$$

From Friedlingstein et al. (2006).

Simulation Identifier	Radiative Coupling: CO_2	Radiative Coupling: Other GHG & aerosols	Biogeochemical Coupling: CO_2	Biogeochemical Coupling: Nitrogen deposition	Biogeochemical Coupling: Land use	Experiment Name
RAD	✓	✓	–	–	–	bcrd
BGC	–	–	✓	✓	–	bdrcs.pftcon
FC	✓	✓	✓	✓	–	bdrd.pftcon

✓ Transient anthropogenic forcing
– Constant pre-industrial (1850) forcing

Climate–Carbon Cycle Drivers (1850–2300)

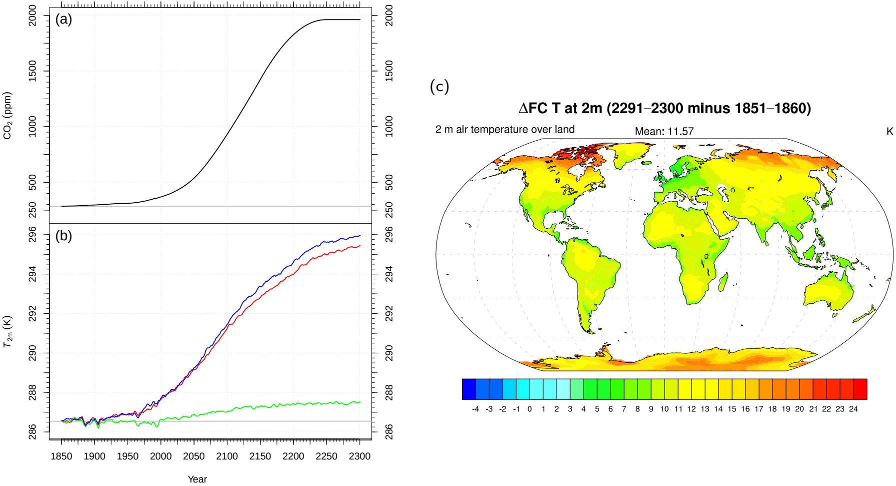

(a) Prescribed atmospheric CO_2 mole fraction was stabilized at 1962 ppm around 2250. (b) 2 m air temperature increased by 9.4°C in **FC**, 8.9°C in **RAD**, and 1.0°C in **BGC** simulations. (c) Mean air temperature over land increased by 11.6°C in the **FC** simulation and approached 25°C at high latitudes.

Net Ocean and Land Carbon Uptake (1850–2300)

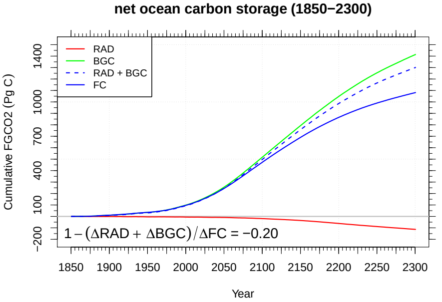

Net ocean carbon storage has a nonlinear response that Schwinger et al. (2014) attributed to surface stratification under climate change that restricted C penetration into intermediate and deep waters.

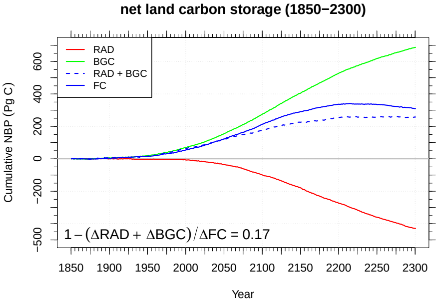

Net land carbon storage also has a nonlinear response, of opposite sign, that has not been explored in ESMs, although Zickfeld et al. (2011) explored similar nonlinear responses in an EMIC. It is driven by larger than expected productivity increases due to positive hydrological and nitrogen mineralization feedbacks.

Ocean and Land Climate–Carbon Sensitivities

The difference between the net ocean carbon storage climate sensitivities, γ_O^{RAD} and $\gamma_O^{\mathrm{FC-BGC}}$, was nearly $-27\ \mathrm{Pg\,C\,K^{-1}}$ and continued to diverge at the end of the 23$^{\mathrm{rd}}$ century.

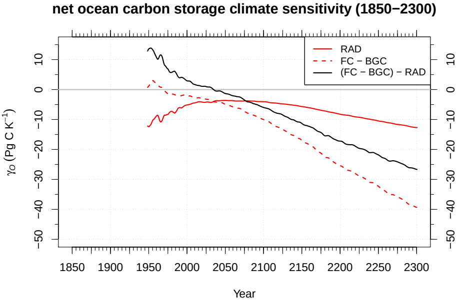

The difference between the net land carbon storage climate sensitivities, γ_L^{RAD} and $\gamma_L^{\mathrm{FC-BGC}}$, peaked at about $10\ \mathrm{Pg\,C\,K^{-1}}$ around 2175 and ended at about $4\ \mathrm{Pg\,C\,K^{-1}}$ at 2300.

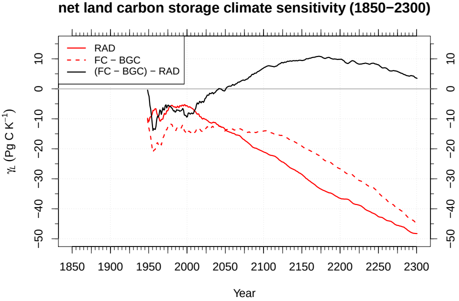

Climate Sensitivities and Climate–Carbon Cycle Gains

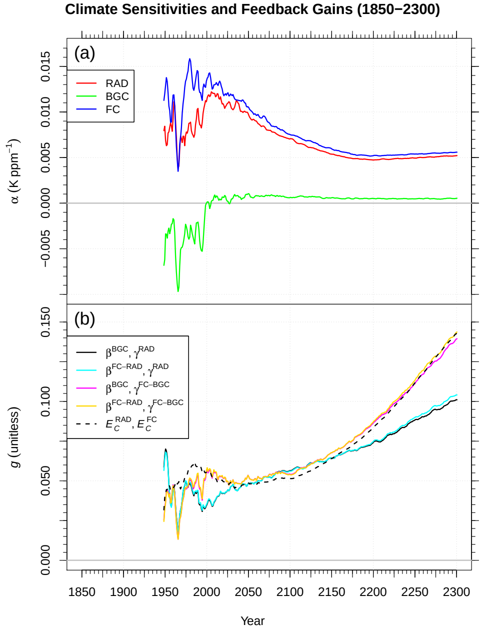

The climate sensitivity, α, for the **FC** simulation was about 0.0056 K ppm^{-1} at the end of the 23rd century.

The climate–carbon cycle gain* (g) clustered around two different values, depending on the method and experiments used to calculate it, and at 2300 was 42% higher when estimated from sensitivity parameters derived from (**FC** − **BGC**) than from **RAD**.

*This gain included effects of aerosols and other greenhouse gases.

Drivers of Nonlinear Terrestrial Uptake Responses

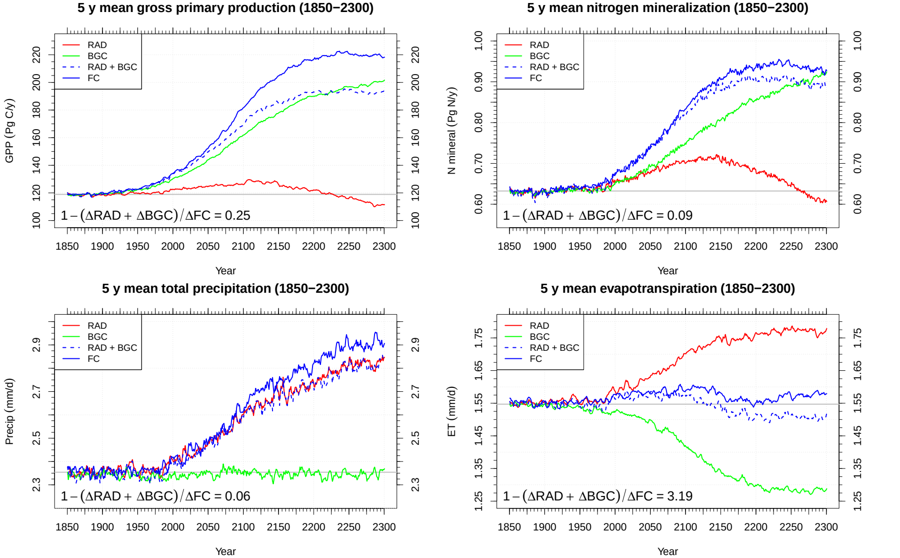

Enhanced gross primary production (GPP) and higher rates of N mineralization, driven by excess precipitation increases and reduced evapotranspiration, led to the nonlinear C uptake response on land under simultaneous climate change and elevated CO_2 levels.

Nonlinear GPP Responses Across Model Experiments

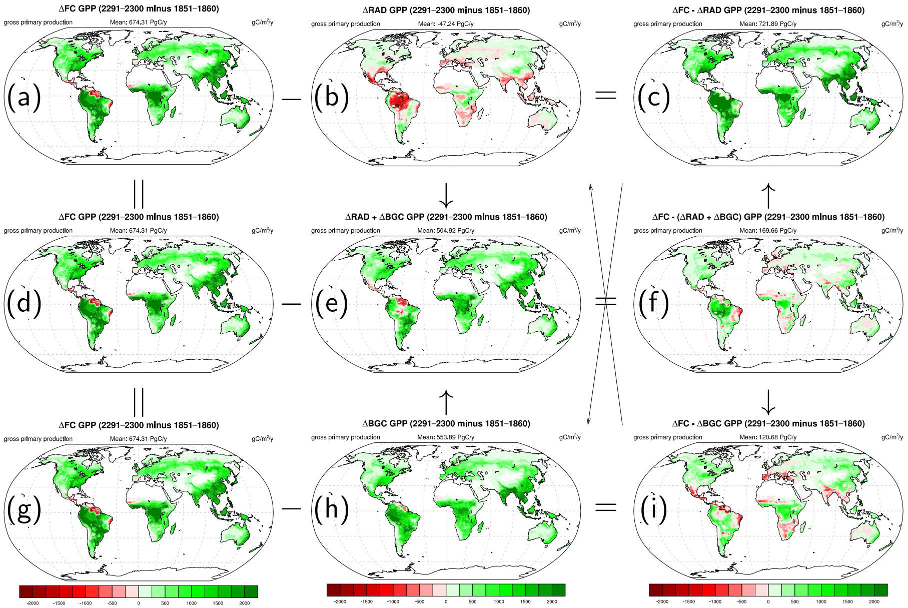

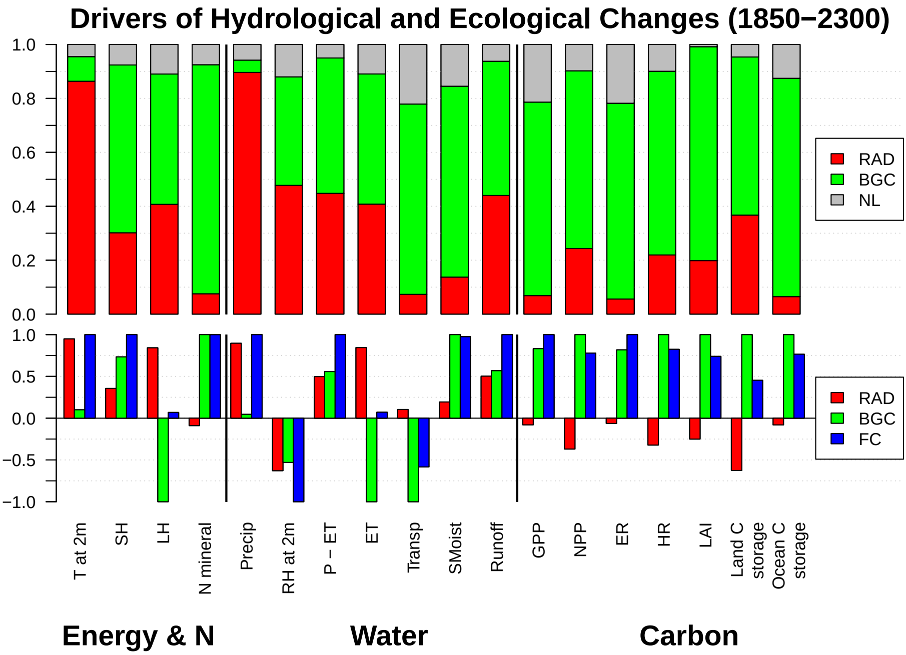

Drivers of Hydrological and Ecological Changes (1850−2300)
RAD
BGC
NL
FC
1.0
0.8
0.6
0.4
0.2
0.0
0.5
−0.5
−1.0
T at 2m
SH
LH
N mineral
Precip
RH at 2m
P − ET
ET
Transp
SMoist
Runoff
GPP
NPP
ER
HR
LAI
Land C storage
Ocean C storage
Energy & N
Water
Carbon

Summary and Conclusions

Question 3

To what degree do the effects of climate change due to warming and CO_2 fertilization in isolation combine linearly?

- **RAD** simulations yielded a net ocean carbon storage climate sensitivity (γ_O) that was weaker and a net land carbon storage sensitivity (γ_L) that was stronger than those diagnosed from **FC** and **BGC** simulations.
  - For the ocean, the nonlinearity was associated with warming-induced weakening of ocean circulation and mixing, which limited exchange of dissolved inorganic carbon between surface and deeper water masses.
  - For the land, the nonlinearity was associated with strong gains in gross primary production in the **FC** simulation, driven by enhancements in the hydrological cycle and increased nutrient availability.
- The feedback gain* (g) at 2300 was 42% higher when estimated from sensitivity parameters derived from (**FC** − **BGC**) than from **RAD**.
- We recommend deriving $\gamma_O^{\mathrm{FC-BGC}}$ and $\gamma_L^{\mathrm{FC-BGC}}$ in future studies.

*This gain included effects of aerosols and other greenhouse gases.

BGC Experiments Planning

Forrest M. Hoffman
forrest@climatemodeling.org

Land Group Simulation Experiments

- Point simulations
  - Representative sites
  - Super sites
  - Fluxnet sites
- Manipulation experiments
  - Litter decomposition
  - Fertilization experiments
  - FACE
  - Warming experiments
- Partially coupled global simulations (AMIP-style)
- Fully coupled regional simulations
- Fully coupled global simulations

V1 Experimental Design

- **Science Question:** What are the nitrogen (N) and phosphorus (P) effects on carbon-climate and carbon-concentration feedbacks in the presence of land use change and N & P deposition trajectories?
- For V1 BGC experiments, we borrowed the Historical + RCP 8.5 simulation protocol with alternative atmospheric CO_2 coupling from CMIP5:
  - Controls: C1 (no down-regulation), C2 (fixed PFT-specific V_{cmax} down-regulation to match PFT-integrate pre-industrial NPP as the mean of C3 and C5
  - C3 (RD-CN), C4 (RD-CNP), C5 (ECA-CN), C6 (ECA-CNP)
  - For each C: control, **BGC coupled**, **RAD coupled**, and **FULL coupled** for 1850–2100 (Historical + RCP 8.5)
- 6 configurations ✕ 4 scenarios ✕ 250 y = 6,000 simulated years
- At 1° the estimated computational cost is 10M core-hours per 100 simulated years, **total allocation cost is estimated at 600M core-hours** (not including spin up)

V2 Experimental Design

- Model experiments should be designed to:
    - Diagnose/quantify the strength and distribution of model biases
    - Demonstrate reduced biases and errors relative to previous model versions
    - Address new science questions or hypotheses
- Model experiments should highlight/test/exercise new V2 features:
    - Demonstrate utility of topographic downscaling
    - Explore lateral subsurface processes
    - Test new hydrological processes with thermal physics and transport
    - Test explicit microbial model, wetland hydrology & biogeochemistry, nutrient storage and transport, alternative nutrient cycling approaches, and dynamic vegetation
    - Investigate agricultural impacts of different crop types
    - Address land use change questions through scenario testing
- We should establish a plan and a schedule to assure we can accomplish all of the experiments we would like to do.

C^4MIP Simulations for CMIP6

The primary focus of the Coupled Climate–Carbon Cycle Model Intercomparison Project (C^4MIP) is to understand and quantify future century-scale changes in land and ocean carbon storage and fluxes. ESM simulations were devised to achieve this:

- idealized experiments to separate and quantify the sensitivity of land and ocean carbon cycle to changes in climate and atmospheric CO_2,
- historical experiments to evaluate model performance and investigate the potential for observational constraints on future projections,
- future scenario experiments to quantify future changes in carbon storage and hence the atmospheric CO_2 concentration and related climate change for given CO_2 emissions.

Experiments are designed to partner with CMIP6 Historical and DECK experiments.

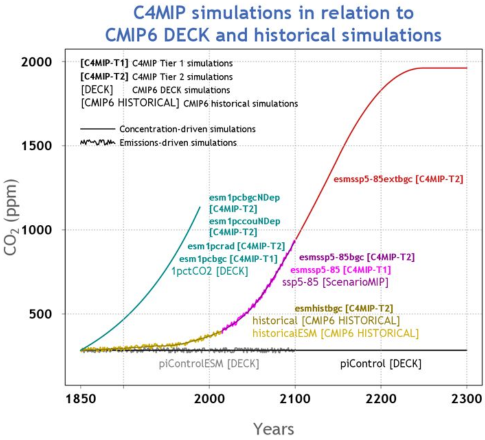

C^4MIP Experiments for CMIP6

Category	Type of Scenario	Emission or Concentration Driven	Coupling Mode	Simulation Years	Short Name	Use by Other MIPS
Tier 1						
1% BGC	Idealized 1% per year CO_2 only, BGC mode	C-driven	CO_2 affects BGC	140	esm1pcbgc	OCMIP, LS3MIP
SSP5-8.5	SSP5-8.5 up to 2100	E-driven	Fully coupled	85	esmssp5-85	ScenarioMIP, LUMIP, OCMIP, LS3MIP
Tier 2						
1% RAD	Idealized 1% per year CO_2 only, RAD mode	C-driven	CO_2 affects RAD	140	esm1pcrad	OCMIP, LS3MIP
1% COU-Ndep	Idealized 1% per year CO_2 only, fully coupled, increasing N-deposition	C-driven	Fully coupled	140	esm1pccou-Ndep	OCMIP

C^4MIP Experiments for CMIP6

Category	Type of Scenario	Emission or Concentration Driven	Coupling Mode	Simulation Years	Short Name	Use by Other MIPS
Tier 2 (continued)						
1% BGC-Ndep	Idealized 1% per year CO_2 only, BGC mode, increasing N-deposition	C-driven	CO_2 affects BGC	140	esm1pcbgc-Ndep	OCMIP
Hist/SSP5-8.5-BGC	Historical + SSP5-8.5 up to 2300, BGC mode	C-driven	CO_2 affects BGC	i. 155 ii. 085 iii. 200	esmhistbgc, esmssp5-85bgc, and esmssp5-85extbgc	ScenarioMIP, OCMIP, LS3MIP, DAMIP

Proposed Coupled Experiments 1

- Idealized experiments designed to quantify carbon cycle feedback sensitivities
  - Idealized 1% per year CO_2, **BGC coupling**, **C-driven**, constant N-dep, aerosols, CH_4 and other GHGs, no crops or LUC or management (140 y)
  - Idealized 1% per year CO_2, **RAD coupling**, **C-driven**, constant N-dep, aerosols, CH_4 and other GHGs, no crops or LUC or management (140 y)
  - Idealized 1% per year CO_2, **FULL coupling**, **C-driven**, constant N-dep, aerosols, CH_4 and other GHGs, no crops or LUC or management (140 y)
- Idealized experiments designed to quantify the influence of nutrient cycles on carbon cycle feedback sensitivities
  - Idealized 1% per year CO_2, **BGC coupling**, **C-driven**, increasing N-dep, aerosols, CH_4 and other GHGs, no crops or LUC or management (140 y)
  - Idealized 1% per year CO_2, **RAD coupling**, **C-driven**, increasing N-dep, aerosols, CH_4 and other GHGs, no crops or LUC or management (140 y)
  - Idealized 1% per year CO_2, **FULL coupling**, **C-driven**, increasing N-dep, aerosols, CH_4 and other GHGs, no crops or LUC or management (140 y)

Proposed Coupled Experiments 2

- Pre-industrial control experiment to quantify residual drift in climate & BGC cycles
  - 500–1000 y control, **FULL coupling**, **C-driven**, constant N-dep, aerosols, CH_4 and other GHGs, no crops or LUC or management (500–1000 y)

Proposed Coupled Experiments 3

- Historical experiments designed to evaluate model performance and investigate emergent constraints
  - Historical CO_2, **BGC coupling**, **C-driven**, increasing N-dep, aerosols, CH_4 and other GHGs, dynamic crops and LUC and management (165 y)
  - Historical CO_2, **RAD coupling**, **C-driven**, increasing N-dep, aerosols, CH_4 and other GHGs, dynamic crops and LUC and management (165 y)
  - Historical CO_2, **FULL coupling**, **C-driven**, increasing N-dep, aerosols, CH_4 and other GHGs, dynamic crops and LUC and management (165 y)
  - Historical CO_2, **BGC coupling**, **E-driven**, increasing N-dep, aerosols, CH_4 and other GHGs, dynamic crops and LUC and management (165 y)
  - Historical CO_2, **RAD coupling**, **E-driven**, increasing N-dep, aerosols, CH_4 and other GHGs, dynamic crops and LUC and management (165 y)
  - Historical CO_2, **FULL coupling**, **E-driven**, increasing N-dep, aerosols, CH_4 and other GHGs, dynamic crops and LUC and management (165 y)

Proposed Coupled Experiments 4

- Future scenario experiments designed to quantify future changes in carbon cycle storage for given CO_2 and land use trajectories
  - SSP5-8.5 to 2100, **BGC coupling**, **C-driven**, increasing N-dep, aerosols, CH_4 and other GHGs, dynamic crops and LUC and management (85 y)
  - SSP5-8.5 to 2100, **RAD coupling**, **C-driven**, increasing N-dep, aerosols, CH_4 and other GHGs, dynamic crops and LUC and management (85 y)
  - SSP5-8.5 to 2100, **FULL coupling**, **C-driven**, increasing N-dep, aerosols, CH_4 and other GHGs, dynamic crops and LUC and management (85 y)
  - SSP5-8.5 to 2100, **BGC coupling**, **E-driven**, increasing N-dep, aerosols, CH_4 and other GHGs, dynamic crops and LUC and management (85 y)
  - SSP5-8.5 to 2100, **RAD coupling**, **E-driven**, increasing N-dep, aerosols, CH_4 and other GHGs, dynamic crops and LUC and management (85 y)
  - SSP5-8.5 to 2100, **FULL coupling**, **E-driven**, increasing N-dep, aerosols, CH_4 and other GHGs, dynamic crops and LUC and management (85 y)

Proposed Coupled Experiments 5

- Extension of future scenario experiments designed to quantify non-linear carbon cycle feedbacks, strengthening of biogeophysical and biogeochemical feedbacks, and shifting strength of ocean and land feedbacks
    - SSP5-8.5 to 2300, **BGC coupling**, **C-driven**, increasing N-dep, aerosols, CH_4 and other GHGs, dynamic crops and LUC and management (200 y)
    - SSP5-8.5 to 2300, **RAD coupling**, **C-driven**, increasing N-dep, aerosols, CH_4 and other GHGs, dynamic crops and LUC and management (200 y)
    - SSP5-8.5 to 2300, **FULL coupling**, **C-driven**, increasing N-dep, aerosols, CH_4 and other GHGs, dynamic crops and LUC and management (200 y)

Total simulated years: 3440–3940 years (not including spin up simulations)

Acknowledgments

U.S. DEPARTMENT OF ENERGY

Office of Science

NSF

This research was supported by the Bigeochemistry–Climate Feedbacks (BGC Feedbacks) Scientific Focus Area, which is sponsored by the Regional and Global Climate Modeling Program in the Climate and Environmental Sciences Division (CESD) of the Biological and Environmental Research (BER) Program in the U.S. Department of Energy Office of Science, and by the National Science Foundation (AGS-1048890). This research used resources of the National Center for Computational Sciences (NCCS) at Oak Ridge National Laboratory (ORNL), which is managed by UT-Battelle, LLC, for the U.S. Department of Energy under Contract No. DE-AC05-00OR22725.

References

R. J. Andres, J. S. Gregg, L. Losey, G. Marland, and T. A. Boden. Monthly, global emissions of carbon dioxide from fossil fuel consumption. *Tellus B*, 63(3):309–327, July 2011. doi:10.1111/j.1600-0889.2011.00530.x.

R. J. Andres, T. A. Boden, F.-M. Bréon, P. Ciais, S. Davis, D. Erickson, J. S. Gregg, A. Jacobson, G. Marland, J. Miller, T. Oda, J. G. J. Olivier, M. R. Raupach, P. Rayner, and K. Treanton. A synthesis of carbon dioxide emissions from fossil-fuel combustion. *Biogeosci.*, 9(5):1845–1871, May 2012. doi:10.5194/bg-9-1845-2012.

P. M. Cox, D. Pearson, B. B. Booth, P. Friedlingstein, C. Huntingford, C. D. Jones, and C. M. Luke. Sensitivity of tropical carbon to climate change constrained by carbon dioxide variability. *Nature*, 494(7437):341–344, Feb. 2013. doi:10.1038/nature11882.

P. Friedlingstein, P. M. Cox, R. A. Betts, L. Bopp, W. von Bloh, V. Brovkin, S. C. Doney, M. Eby, I. Fung, B. Govindasamy, J. John, C. D. Jones, F. Joos, T. Kato, M. Kawamiya, W. Knorr, K. Lindsay, H. D. Matthews, T. Raddatz, P. Rayner, C. Reick, E. Roeckner, K.-G. Schnitzler, R. Schnur, K. Strassmann, S. Thompson, A. J. Weaver, C. Yoshikawa, and N. Zeng. Climate–carbon cycle feedback analysis, results from the C^4MIP model intercomparison. *J. Clim.*, 19(14):3373–3353, July 2006. doi:10.1175/JCLI3800.1.

A. Hall and X. Qu. Using the current seasonal cycle to constrain snow albedo feedback in future climate change. *Geophys. Res. Lett.*, 33(3):L03502, Feb. 2006. doi:10.1029/2005GL025127.

F. M. Hoffman, J. T. Randerson, V. K. Arora, Q. Bao, P. Cadule, D. Ji, C. D. Jones, M. Kawamiya, S. Khatiwala, K. Lindsay, A. Obata, E. Shevliakova, K. D. Six, J. F. Tjiputra, E. M. Volodin, and T. Wu. Causes and implications of persistent atmospheric carbon dioxide biases in Earth System Models. *J. Geophys. Res. Biogeosci.*, 119(2):141–162, Feb. 2014. doi:10.1002/2013JG002381.

S. Khatiwala, T. Tanhua, S. Mikaloff Fletcher, M. Gerber, S. C. Doney, H. D. Graven, N. Gruber, G. A. McKinley, A. Murata, A. F. Ríos, and C. L. Sabine. Global ocean storage of anthropogenic carbon. *Biogeosci.*, 10(4):2169–2191, Apr. 2013. doi:10.5194/bg-10-2169-2013.

Emergent Constraint Developed from CMIP5 ESMs

An emergent constraint based on carbon inventories was applied to future atmospheric CO_2 projections from CMIP5 ESMs.

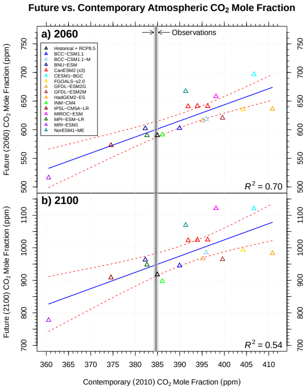

- Much of the model-to-model variation in projected CO_2 during the 21st century is tied to biases that existed during observational era.
- Model differences in the representation of concetration–carbon feedbacks and other slowly changing carbon cycle processes appear to be the primary driver of this variability.
- Range of temperature increases at 2100 slightly reduced, from $5.1 \pm 2.2^\circ$C for the full ensemble, to $5.0 \pm 1.9^\circ$C after applying the emergent constraint.

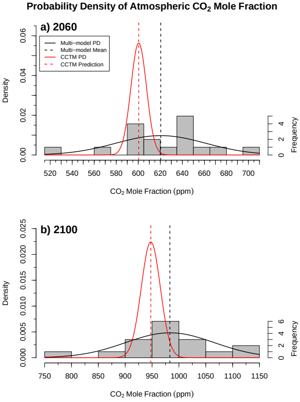

Best estimate using Mauna Loa CO_2

At 2060: 600 $\pm$ 14 ppm, 21 ppm below the multi-model mean
At 2100: 947 $\pm$ 35 ppm, 32 ppm below the multi-model mean

Hoffman, Forrest M., James T. Randerson, Vivek K. Arora, Qing Bao, Patricia Cadule, Duoying Ji, Chris D. Jones, Michio Kawamiya, Samar Khatiwala, Keith Lindsay, Atsushi Obata, Elena Shevliakova, Katharina D. Six, Jerry F. Tjiputra, Evgeny M. Volodin, and Tongwen Wu. February 2014. "Causes and Implications of Persistent Atmospheric Carbon Dioxide Biases in Earth System Models." *J. Geophys. Res. Biogeosci.*, 119(2):141–162. doi:10.1002/2013JG002381. *Most downloaded JGR-B paper for February 2014.*

Model inventory comparison with Sabine et al. (2004)

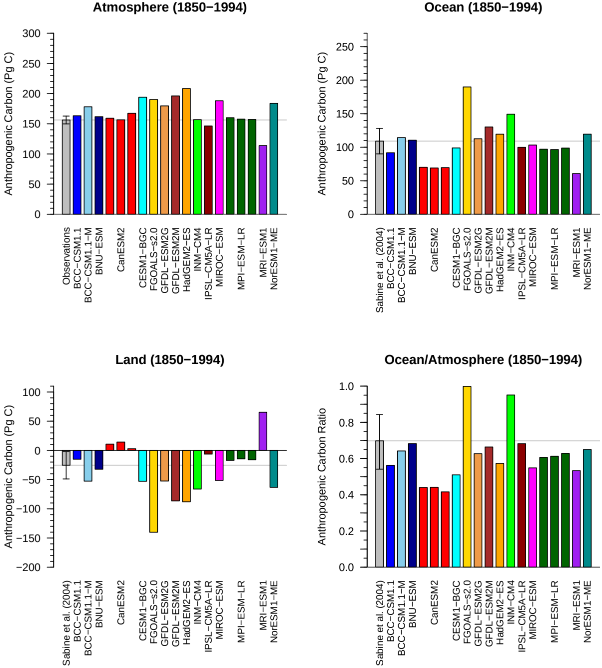

Implications for CO_2, Radiative Forcing, and Temperature

Model	CO_2 Mole Fraction (ppm)			Radiative Forcing ($W\,m^{-2}$)			Cumulative ΔT (°C)			ΔT Bias (°C)		
	2010	2060	2100	2010	2060	2100	2010	2060	2100	2010	2060	2100
BCC-CSM1.1	390	603	945	1.70	4.03	6.43	0.97	2.39	4.02	0.03	0.02	−0.01
BCC-CSM1.1-M	396	619	985	1.78	4.16	6.65	1.04	2.49	4.16	0.10	0.12	0.13
BNU-ESM	382	602	963	1.59	4.02	6.53	0.90	2.33	4.07	−0.04	−0.04	0.04
CanESM2 r1	394	641	1024	1.75	4.36	6.86	0.98	2.58	4.30	0.04	0.21	0.27
CanESM2 r2	392	641	1023	1.72	4.35	6.85	0.98	2.57	4.30	0.04	0.20	0.27
CanESM2 r3	396	641	1025	1.78	4.35	6.87	1.01	2.58	4.30	0.07	0.21	0.27
CESM1-BGC	407	697	1121	1.92	4.80	7.34	1.12	2.85	4.64	0.18	0.48	0.61
FGOALS-s2.0	404	636	993	1.89	4.31	6.70	1.09	2.57	4.23	0.15	0.20	0.20
GFDL-ESM2G	395	616	967	1.77	4.14	6.56	1.04	2.49	4.12	0.10	0.12	0.09
GFDL-ESM2M	400	621	964	1.83	4.18	6.54	1.09	2.52	4.13	0.15	0.15	0.10
HadGEM2-ES	411	636	983	1.98	4.31	6.64	1.18	2.60	4.20	0.24	0.23	0.17
INM-CM4	386	591	897	1.64	3.92	6.15	0.92	2.36	3.86	−0.02	−0.01	−0.17
IPSL-CM5A-LR	375	573	908	1.48	3.75	6.22	0.86	2.21	3.87	−0.08	−0.16	−0.16
MIROC-ESM	398	658	1121	1.81	4.50	7.35	1.06	2.67	4.58	0.12	0.30	0.55
MPI-ESM-LR r1	383	590	948	1.60	3.91	6.45	0.95	2.31	4.03	0.01	−0.06	0.00
MRI-ESM1	361	516	778	1.28	3.20	5.39	0.74	1.89	3.33	−0.20	−0.48	−0.70
NorESM1-ME	391	667	1070	1.72	4.57	7.09	0.98	2.68	4.46	0.04	0.31	0.43
Multi-model Mean	392	621	980	1.72	4.18	6.63	1.00	2.48	4.17	0.06	0.11	0.14
CCTM Estimate	385	600	948	1.62	4.01	6.45	0.94	2.37	4.03	—	—	—
Historical + RCP 8.5	385	590	917	1.63	3.91	6.27	0.94	2.32	3.93	0.00	−0.05	−0.10

Century-by-Century Carbon & Temperature Changes

Variable	Time (year) 2000	2100	2200	2300
$[CO_2]_A$ (ppm)	369	936	1829	1962
Variable	**Time Period (years) 1850–2000**	**1850–2100**	**1850–2200**	**1850–2300**
$\Delta T_{2\,\mathrm{m}}^{\mathrm{RAD}}$ (K)	1.13	4.76	7.46	8.90
$\Delta T_{2\,\mathrm{m}}^{\mathrm{BGC}}$ (K)	0.10	0.50	0.87	0.99
$\Delta T_{2\,\mathrm{m}}^{\mathrm{FC}}$ (K)	1.19	4.92	8.11	9.41
$\Delta C_O^{\mathrm{RAD}}$ (Pg C)	−6	−19	−62	−113
$\Delta C_O^{\mathrm{BGC}}$ (Pg C)	100	519	1050	1414
ΔC_O^{FC} (Pg C)	97	475	866	1082
$\Delta C_L^{\mathrm{RAD}}$ (Pg C)	−8	−100	−275	−430
$\Delta C_L^{\mathrm{BGC}}$ (Pg C)	69	276	529	687
ΔC_L^{FC} (Pg C)	55	213	336	309
E_C^{RAD} (Pg C)	167	1265	2948	3023
E_C^{BGC} (Pg C)	349	2180	4862	5663
E_C^{FC} (Pg C)	331	2072	4486	4955

Climate–Carbon Cycle Feedback Parameters and Gains

Parameter	Time Period (years)			
	1850–2000	1850–2100	1850–2200	1850–2300
α (K ppm^{-1})	0.0140	0.0075	0.0052	0.0056
β_O^{BGC} (Pg C ppm^{-1})	1.19	0.80	0.68	0.84
$\beta_O^{\mathrm{FC-RAD}}$ (Pg C ppm^{-1})	1.23	0.76	0.60	0.71
β_L^{BGC} (Pg C ppm^{-1})	0.84	0.42	0.34	0.41
$\beta_L^{\mathrm{FC-RAD}}$ (Pg C ppm^{-1})	0.72	0.48	0.39	0.44
γ_O^{RAD} (Pg C K^{-1})	−5.10	−4.06	−8.26	−12.69
$\gamma_O^{\mathrm{FC-BGC}}$ (Pg C K^{-1})	−2.22	−10.06	−25.47	−39.37
γ_L^{RAD} (Pg C K^{-1})	−5.70	−21.09	−36.54	−48.25
$\gamma_L^{\mathrm{FC-BGC}}$ (Pg C K^{-1})	−15.00	−14.05	−26.69	−44.77
$g(\beta^{\mathrm{BGC}}, \gamma^{\mathrm{RAD}})$	0.035	0.056	0.075	0.101
$g(\beta^{\mathrm{FC-RAD}}, \gamma^{\mathrm{RAD}})$	0.036	0.056	0.075	0.104
$g(\beta^{\mathrm{BGC}}, \gamma^{\mathrm{FC-BGC}})$	0.057	0.054	0.087	0.139
$g(\beta^{\mathrm{FC-RAD}}, \gamma^{\mathrm{FC-BGC}})$	0.058	0.053	0.087	0.144
$g(E_C^{\mathrm{RAD}}, E_C^{\mathrm{FC}})$	0.056	0.051	0.084	0.143